Defect Categorization of Ribbon Blender Worm Gearbox Worm Wheel and Bearing Based on Artificial Neural Network

Indexed by:
Web of Science Group

Raghavendra Rajendra Barshikar[a,*], Harshvardhan P. Ghongade[b], Anjali A. Bhadre[c], Harjitkumar U. Pawar[d], Harshal S. Rane[d]

[a] Department of Mechanical Engineering, MET's Institute of Engineering, India
[b] Department of Mechanical Engineering, Bramha Valley College of Engineering and Research Institute, India
[c] Department of Computer Engineering, Brahma Valley College of Engineering and ResearchInstitute, India
[d] Department of Mechanical, S.N.D. College of Engineering & Research Centre, India

Highlights

- Study of ribbon blender worm gearbox vibration signatures at different condition.
- Usefulness of categorising coalesced i.e. combined worm gear and bearing faults in enhanced productivity, flexibility and agility.
- Advantages of ANN for defect categorization over SVM.

Abstract

There is a demand for worm gearboxes in diversified industrial fields that include machinery such as escalators, ribbon blenders, pulverisers, bowl mills, etc. because of their peculiar characteristics like torque and quick retardation. The most commonly occurring defects in a worm gear box are scratches that develop in the worm gear and in bearings. Early defect categorization is required to prevent a sudden breakdown that would decrease production. The defect is depicted in different cases, which include defects in the gear tooth and the outer and inner races of the bearing. In another case, the defect is considered in the gear tooth as well as the bearing. The severity is designated using the ANN. The experiments were performed under these conditions with a good worm gearbox to capture vibration response signatures. Using these values as an input to the ANN, the model is trained. Experimental results show that vibration amplitude increases with fault progression in the worm gearbox, and the trained ANN model effectively categorizes worm gearbox faults with an accuracy of 97.12%.

Keywords

combine worm wheel–bearing, defect, vibration, ANN, RMS, skewness.

1. Introduction

Catastrophic failure of rotating machinery can results in decreased product quality, increased unexpected maintenance cost, and health hazards for workers. The gearbox's predictive maintenance or condition-based maintenance improves performance, dependability, safety, and productivity while reducing maintenance costs and the risk of a machine stopping suddenly [1]. Predictive maintenance requires accurate defect identification, analysis, categorization, and severity. Various preventative maintenance techniques, include vibration monitoring, motor current signature monitoring, temperature monitoring, and sound monitoring [2-4]. Vibration monitoring is a more popular technique for locating gearbox faults out of these options. There has been little study on using vibration monitoring to diagnose coalesced defects in gearboxes [5]. Shafts, gears, bearings, casings, keys, and couplings are some of the parts that make up a gearbox. Gear and bearings are

(*) Corresponding author.
E-mail addresses: R. Barshikar (ORCID: 0000-0002-3343-8688) raghavendrabarshikar@gmail.com, H. P. Ghongade (ORCID: 0000-0001-6840-3904) ghongade@gmail.com, A. Bhadre (ORCID: 0009-0009-0734-2402) anjalibhadre38@gmail.com, H. U. Pawar (ORCID: 0000-0002-3744-5471) harjitpawar1100@gmail.com, H. S. Rane (ORCID: 0000-0001-9953-7235) harshal17rane@gmail.com,

crucial parts of this component set. When a fault is present in many gearbox components, the vibration signature is different from that of the fault when it is present in a single gearbox component [6]. In case of fault analysis based on vibration monitoring, the signals captured by vibration measuring instruments are altered by various sources like structure-prone vibrations, electromagnetic interference, etc. Therefore, the results of vibration monitoring would mislead the exact condition of the gearbox [7]. Therefore, the first step in fault analysis is to distinguish between the signal generated by the genuine component vibration and the contaminated signal. Separating gear and bearing vibration signatures from polluted vibration signatures needs the denoising technique [8]. The denoising technique needs to be used to differentiate gearbox vibration signatures from polluted vibration signatures [9]. To de-noise the polluted vibration signatures, a variety of de-noising algorithms were used, including residual Convolution Neural Networks (ResNet) [10], wavelet threshold (WT) denoising [11], correlation analysis (CA), variational mode decomposition (VMD) [12] and the wavelet transform as a basis, denoising [13]. When the characteristic rotational frequency, such as gear mesh frequency or shaft rotational frequency, is less than 100 Hz, the wavelet denoising technique by Mishra et al. [14] is appropriate. Turbines, aeroplanes, presses, mines, rolling mills, blending machines, machine tools, conveyors, and escalators all use worm gearboxes as essential parts. At various loads and speeds, the worm gearbox's worm wheel and bearings developed defects such as tooth fracture, corrosion, scratches, and small holes. Early identification and categorization of worm gearbox problems are necessary to prevent a sudden breakdown, harm to people, loss of manufacturing, and financial loss [15]. Because the worm gear material is often softer than the worm screw's, it wears down or gets pitted when sliding in a worm gearbox. [16]. Babu et al. [17] used temperature response to track the state of a worm gearbox under different loads, speeds, and oil levels. The result shows that temperature increases with the deterioration of the worm wheel condition. In the case of a single-start worm gear, oil depth and oil temperature influence churning power loss [18]. It is alarming that the worm gearbox's worm gear has failed. Due to the complexity of acquiring the worm gearbox's vibration signature, very few studies have been conducted on

the defect diagnosis of worm gearboxes using vibration monitoring [19]. The health of the lubricated worm gear can be monitored by employing vibration and sound measurements, and runtime defects can be diagnosed [20]. Vibration analysis-based pitting fault diagnostics of worm gearboxes are covered by Elasha et al. [21]. The assortment of faults is a crucial segment in the diagnosis of machine health condition monitoring. Recent techniques like ANN, CNN, and support vector machines can be of immense help. It is found reported that back propagation multilayer perceptron approach has been implemented and it found that it has given a fair accuracy. This method was found suitable to identify the pitting faults and their severity [22]. The ANN method is applicable to a number of tasks, including categorisation, seriousness, speed recognition, picture identification, and the approximation of random functions [23]. The final result demonstrates that the suggested ANN accurately categorises pitting fault severity. ANN was employed by Barshikar et al. [24] to examine vibration response and find worm gearbox defects. As a result, 92.2% of defects are correctly identified by the ANN model. Agrawal et al. [25] utilized the approaches of ANN and SVM. They focused on the identification and categorization of faults in rolling element bearings. This method reported fair accuracy in the range of 98% to 100%. [26]. Karpat et al. [26] implemented a conventional neural network (CNN) to distinguish rolling element bearing defects in wind turbines. According to Niaki et al. [27], feed-forward artificial neural networks (FANN) can satisfactorily and reliably predict the current condition of helical gearboxes. Similarly, Kane et al. [28] investigated the utility of ANN for fault identification and categorization in spur gear, and various faults were introduced in the gear tooth geometry. For this analysis, he used acoustics, vibration, and psycho-acoustic signals. Attoui et al. [29] analysed the vibrations associated with faults occurring in the outer, ball, and inner races at various rotational frequencies (28.83, 29.16, 29.6, and 30 Hz). On a parallel line, for conducting fault detection experimental trials, plenty of things are needed in the laboratory, which include artificial defect size, speed variation, and load. The ANN model for fault diagnosis of various industrial rotating machinery was found to be effective and suitable. Recent studies use response surface methodology (RSM) and design of experiments (DOE) to create experimental trials and assess vibration signature

responses for defect identification in bearings and gears. Ammar et al. [31] developed the technique to prognosticate the working life of bearings using a laboratory experimental test rig. The developed technique is based on vibration signals, auto-regressive moving average (ARMA), and response surface methodology (RSM). Mishra et al. [32] focused on defect investigation of rotor-bearing assemblies utilising vibration monitoring in conjunction with statistical analysis. Statistical analysis is based on three-level full factorial design and response surface methodology. The measured vibration data was effectively and reliably optimized by using RSM ANOVA and regression based mathematical model [33-34].

During the study and investigation of the worm gearbox, it was found that the fault has been considered on one of the parts while all the remaining parts were intact. It leads to the inference that there is scope for study by considering two faults in different parts at a time.

In the current research, a feed forward back propagation ANN model has been proposed for categorising coalesced, i.e., combined worm gear and bearing faults. The research is unique in that it presents coalesced worm wheel-bearing fault analysis. By employing a wire electrical discharge machining and

a bench machine, defects were intentionally produced in the worm gear bearing's outer race, inner race, and worm gear tooth, respectively. Implementing an FFT analyzer, vibration signatures for various fault states were recorded. To train the ANN model, eight statistical parameters were recovered. To categorise defects and severity of worm gear and bearing, Matlab is used to train an ANN model.

There are three sections in the present research paper: method, discussion of the findings, and conclusion. The methodology section presents experiments performed by using the OR34 FFT analyser to capture the vibration signatures, extraction of statistical parameters, and ANN model.

The outcome of the research and its summary are presented in the conclusion section.

2. Methodology

This section illustrates, the test rig utilized for experimentation and training of the ANN model.

2.1 Laboratory experimental test rig

Fig. 1 depicts the block diagram of the experimental setup.
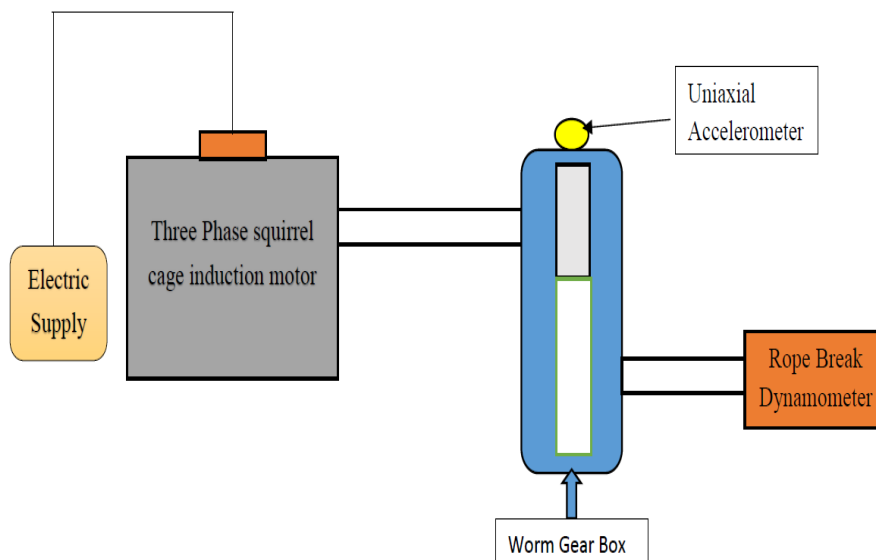
Fig. 1. Block diagram of experimental setup.

For the experimental trials, a constant input speed of 2880 RPM was applied to the worm gearbox with a gear ratio of 1/15. A double-start worm composed of profile-ground steel and case-hardened steel, along with a shell-cast ZCuSn12 bronze worm wheel with 30 teeth, make up the worm gearbox.

A variable-frequency drive is utilized to maintain the worm gearbox's speed. The rope break dynamometer applies the load to the gearbox, and the load cell measures it. In current experiments, the RSM Box-Behnken design [24] is implemented to design experimental trials for three levels with

four variables, as illustrated in Table 1. In the present study, artificial defects were created on worm gear and bearing inner and outer races, as in [24]. The example of an artificially created fault is shown in Figure 2. Figure 3 presents the intact worm gear and worm gear bearing. The response of a system in an experimental setup is measured in terms of vibrations in the frequency domain. Vibration response correlates with the rotating element frequencies, such as gear mesh frequency, outer race bearing pass frequency, and inner race bearing pass frequency, which are excellent indicators of gearbox defect existence [4, 19] when used in the diagnosis of gearbox faults. Worm gear gear mesh frequency, outer race worm gear bearing pass frequency, and inner race worm gear bearing pass frequency, as determined in [24], are all equal to 96 Hz, 15.85 Hz, and 22.54 Hz, respectively.

(a)

(b)

(c)

(d)
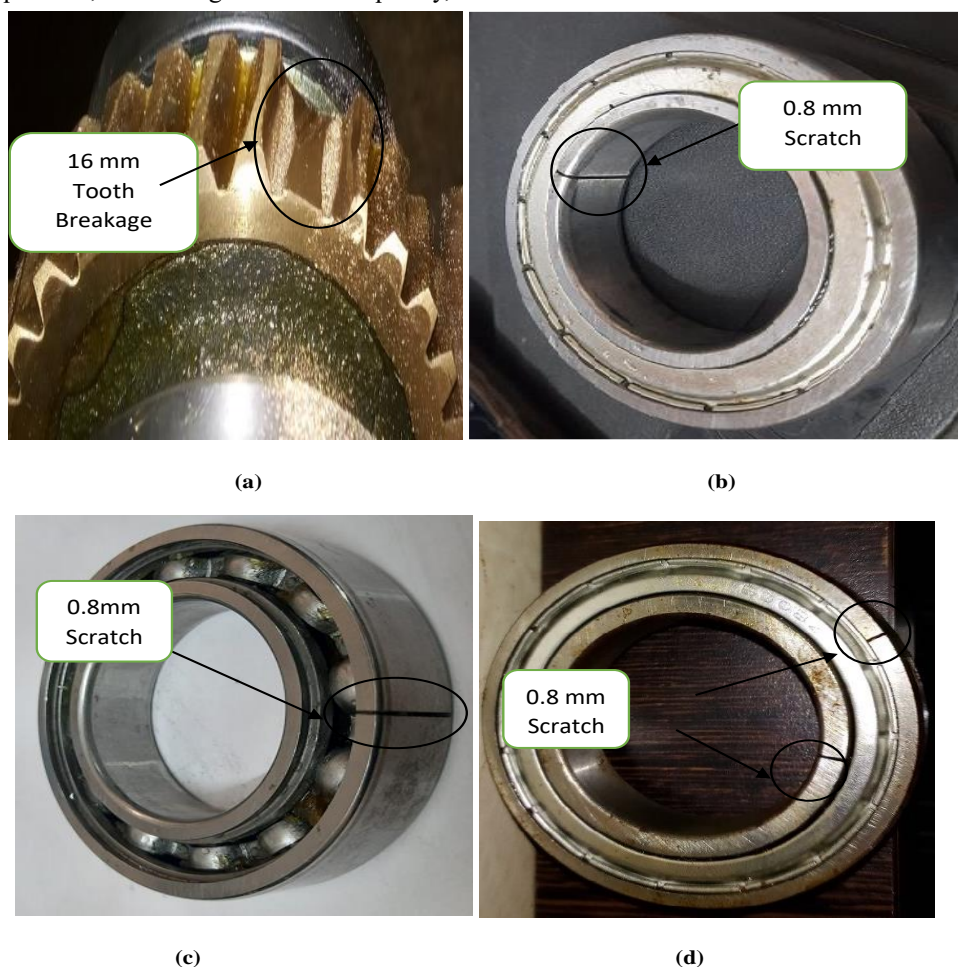
Fig. 2. Defects in (a) worm gear (b) bearing inner race (c) bearing outer race (d) bearing inner and outer race.

(a)

(b)

Fig. 3. Good condition (a) worm gear bearing (b) worm gear.

Table 1. Variables and their values reported in [24].

Notation	Independent parameters	Initial value	Intermediate value	Final value
IR	Bearing inner race faulty	0	0.4 mm	0.8 mm
OR	Bearing outer race faulty	0	0.4 mm	0.8 mm
WW	Worm gear tooth breakage	0	8 mm	16 mm
LOAD	Load applied	10 Kg	15 Kg	20 Kg

2.2. Vibration signature collection with the OR 34 FFT analyzer

The experiments were performed for intact and twenty-seven fault conditions in a gearbox. The vibration response of the system during the experiments was recorded using 4 input FFT analyser and one directional accelerometer. According to Umutu et al. [22], in current experiments, the accelerometer is positioned radially, as illustrated in Fig. 4, for better results.
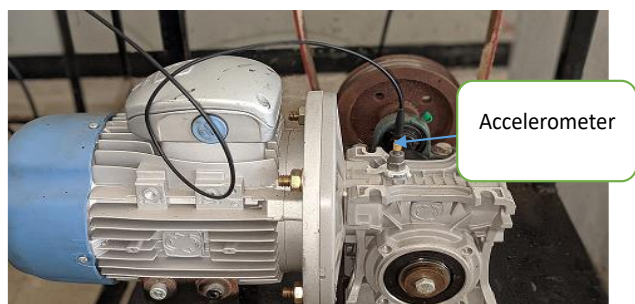
Fig. 4. Accelerometer position.

The OR 34 FFT analyzer is compatible with the NVGate V10.00 software [24]. Based on the available literature, for slow rotational speeds and characteristic rotational frequencies less than 100 Hz, the wavelet denoise method based on the biorthogonal sigmoid thresholding algorithm [14, 24] is implemented to reconstruct contaminated vibration signatures, which may include other components' vibration and noise. NVGate V10.00 software is utilized to perform wavelet denoising. The vibration responses are recorded in the frequency window are corrected by implementing the denoised technique, which leads to the extraction of eight crucial statistical indicators, including standard deviation, variance, skewness, peak to peak, kurtosis, RMS, mean, and crest factor [19, 24]. The OR34 FFT analyzer NVGate software immediately provides RMS statistical parameter values. The Excel data analysis tool calculates the remaining statistical parameters. The trained ANN model receives these parameters as input. The combined worm wheel and bearing defect is located and categorised by the ANN model.

2.3. Technique of artificial neural network

Conceptually, an artificial neural network mimics the human brain to provide solutions to complex situations and challenging problems. The link between the input-output parameters and the training procedure is the foundation of ANN. Multilayer perceptron with feed-forward and backward propagation is, compared to other ANN algorithms, ANN is more widely used [22-25]. Therefore, it has been employed in this study to classify the worm gearbox defects that are present. The figure 5 shows the ANN for the feed forward back propagation multilayer perceptron. There are three layers, which include the initial, intermediate, and final layer. Eight nodes make up the input layer since the ANN model is trained using eight frequency domain statistical parameters, and eight to twelve nodes make up the hidden layer. There are four classification nodes used for fault classification in the output layer. Their output target values are with the range of 0 to 1.
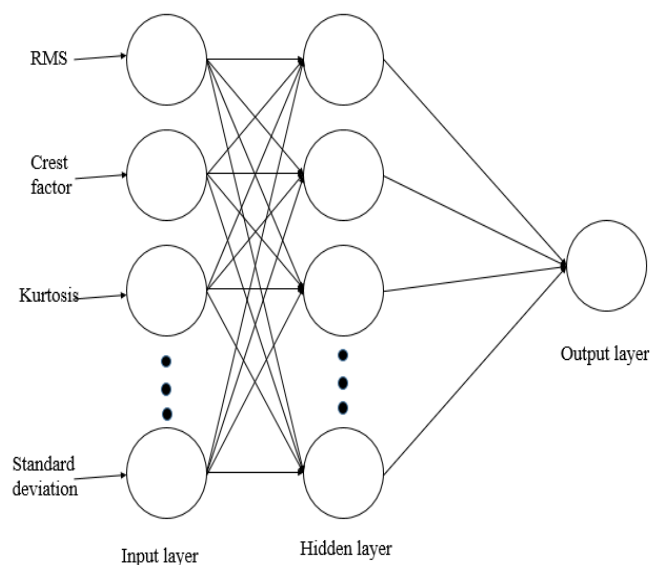
Fig. 5. Structure used in technique of artificial neural network.

Table 2 shows the algorithms employed in this study to

develop an effective ANN model for present experiments [24]. While employing the technique of neural network, the model was trained using the toolbox in MATLAB. The initial weights and biases of ANNs are determined at random. There were 336 inputs utilized for the ANN model. Training, testing, and validation are the three categories into which the ANN model is divided. Out of the total data, 70% was used for training while testing and validation, each was done using 15% of the data [22, 24-25]. After training ANN model; their performance are check. Performance of trained ANN model is based on mean square error (MSE) and regression R value. MSE is the average square difference between output and target. Lower MSE value is better. Regression R value is measure the correlation between output and target. When R value is near to 1 means close relationship. On the other hand R value is equal to 0 means random relationship.

Table 2. Various ANN algorithms for classifying faults.

Initial layer	Intermediate layer	Final layer	Architecture
8	8	4	Bayesian architecture (trainbr)
	10		
	12		
	8		Scaled conjugate gradient architecture (trainscg)
	10		
	12		
	8		Levenberg- Marquardt architecture (trainlm)
	10		
	12		

3. Discussion of the Findings

3.1. Identification potential of de-noised vibration amplitude

The experiments were performed, and the vibration signatures were captured and denoised for various working conditions, as mentioned in Table 2. These include the response of an intact gearbox to various faults, as shown in figures 6 -18. The condition of the gearbox was analyzed by comparing the denoised signal of intact and faulty conditions. These responses were considered at the gear mesh frequency of the worm gear and the pass frequency at the outer and inner races. The loading conditions during the experiments were 10 Kg, 15 Kg, and 20 Kg, respectively. Figure 6 shows healthy worm gearbox vibration signatures for 10 Kg, 15 Kg, and 20 Kg, respectively. Even though the worm gearbox is brand new, it shows some vibration response corresponding to the gear mesh frequency. Figure 7 (a) and (b) show that, even though the defect was on the bearing outer race, there is a slight increase in the vibration response that corresponds to the gear mesh frequency of the worm wheel. Conversely, when the defect is on the bearing inner race, there is a significant increase in the vibration response that corresponds to the gear mesh frequency of the worm wheel. Figure 7 (c) shows that effect of faulty worm wheel on bearing outer race and bearing inner race. When defect occurs on worm wheel teeth, there is slight increase in vibration amplitude of bearing corresponding to outer race elements pass frequency, inner race elements pass frequency.
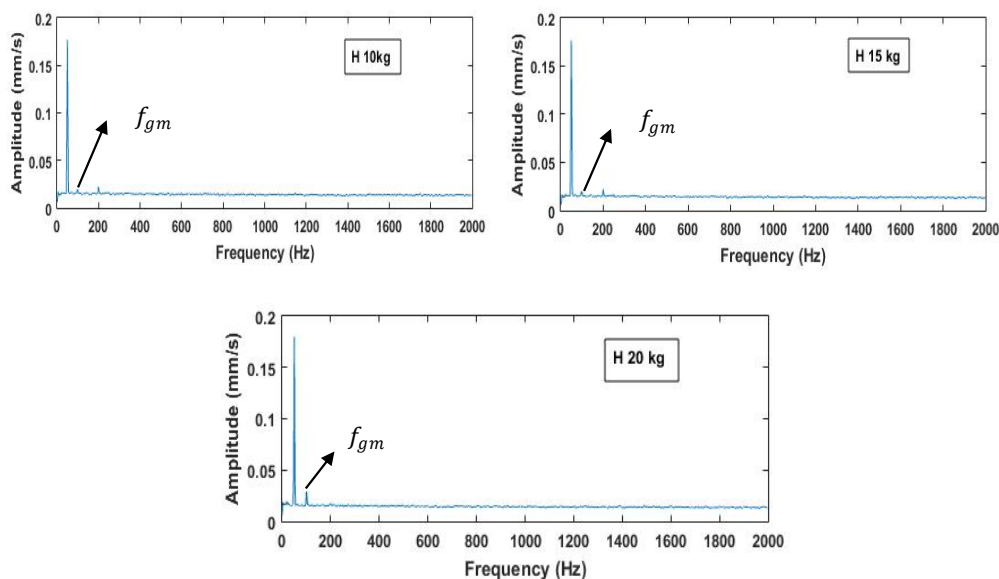
Fig. 6. Denoised frequency domain vibration response of a good worm gearbox (with an output speed of 192 rpm).
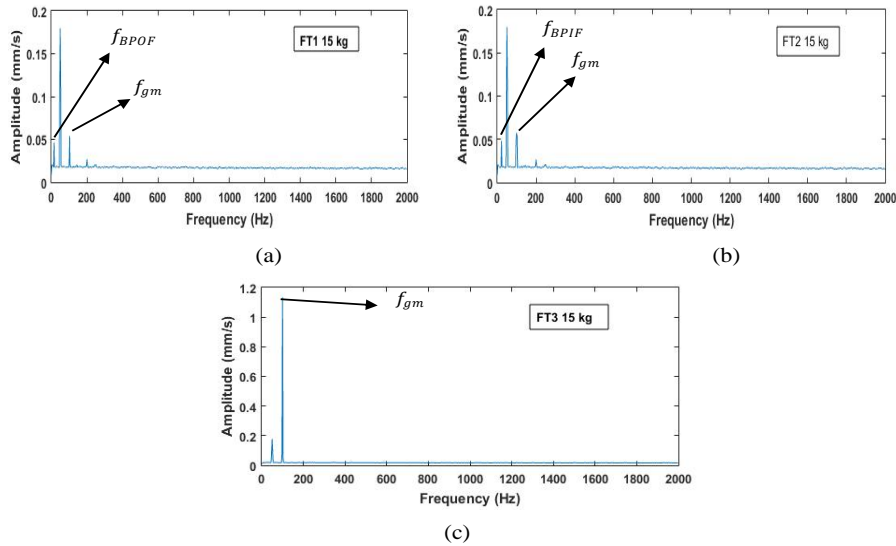
Fig. 7. Denoised frequency domain vibration response of FT1, FT2 and FT3 (with an output speed of 192 rpm).

The vibration signature for fault types FT4, FT5, and FT6 is displayed in Figures 8 and 9. As the load increases from 10 kg to 20 kg, as seen in Figure 8(a) and (b), the vibration amplitude increases. Similar patterns also show in figure 9 that when a bearing outer race and inner race fault together, the vibration amplitude increases significantly and is correlated with the worm wheel's gear mesh frequency. As shown in figures 10 to 11, when a worm wheel and bearing outer race are both faulty, the amplitude of the worm wheel vibration rises as the bearing outer race defect gets more severe. When a worm wheel and bearing inner race are both defective, an identical pattern is seen,

as shown in figures 12 to 13. Figure 14 to Figure 18 show vibration signature for coalesced faults type FT13 to FT19. Similar pattern is observed that worm wheel vibration amplitude increasers more and vibration amplitude changes with load. It has been observed that the vibration response of a faulty worm gearbox increases as the load increases. While the same vibrational behaviour is not recorded for the fault on bearing outer race. It is noticed that vibration levels increase significantly at the worm gear, corresponding to the mesh frequency when there is a fault in the inner race. [22].
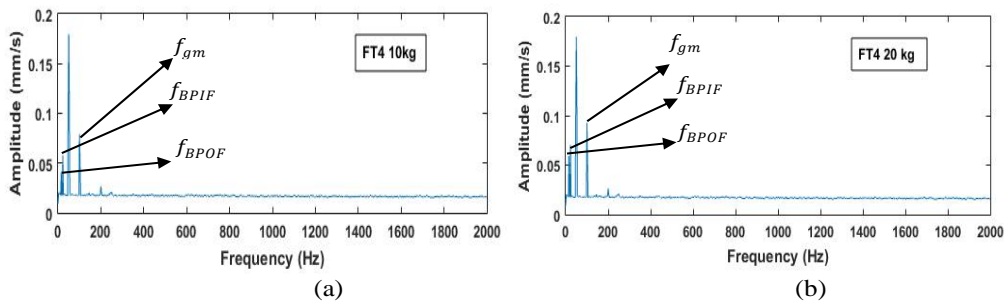
Fig. 8. Denoised frequency domain vibration response of FT4 (with an output speed of 192 rpm).
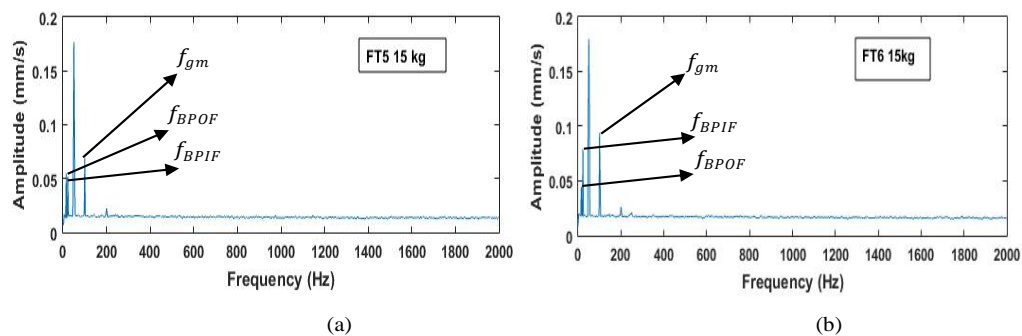
Fig. 9. Denoised frequency domain vibration response of FT5 & FT6 (with an output speed of 192 rpm).
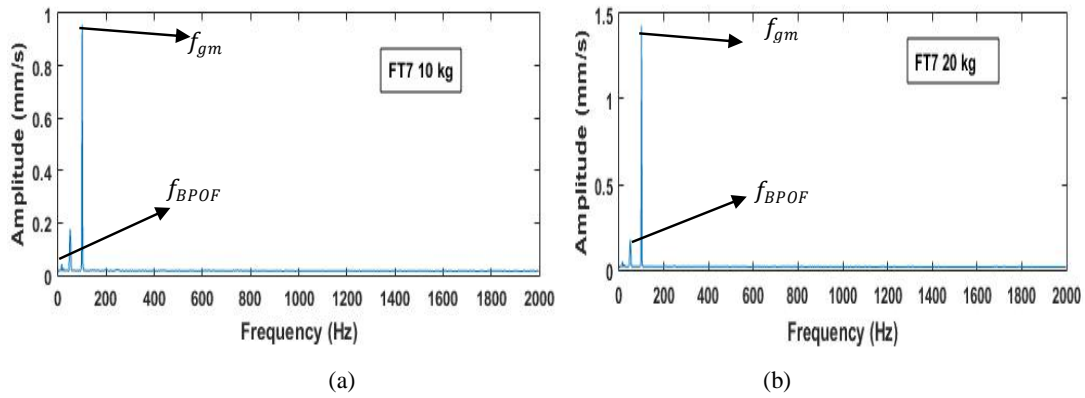
Fig. 10. Denoised frequency domain vibration response of FT7 (with output speed =192 rpm).
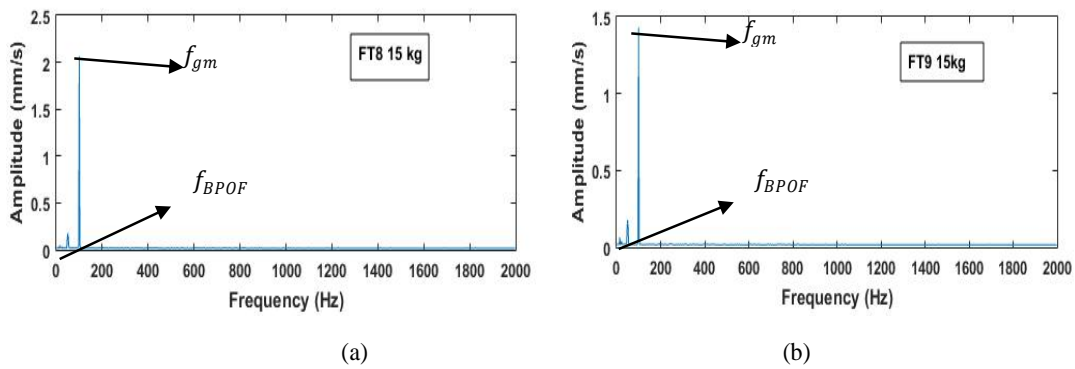
Fig. 11. Denoised frequency domain vibration response of FT8, FT9 (with an output speed of 192 rpm).
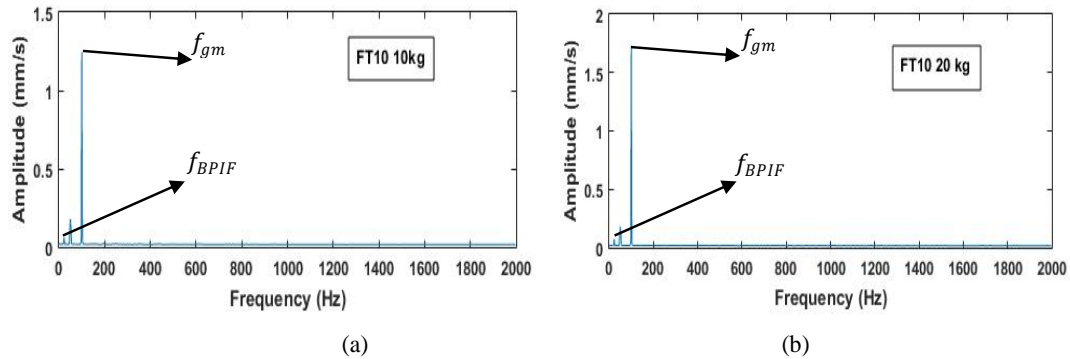
Fig. 12. Denoised frequency domain vibration response of FT10 (with an output speed of 192 rpm).
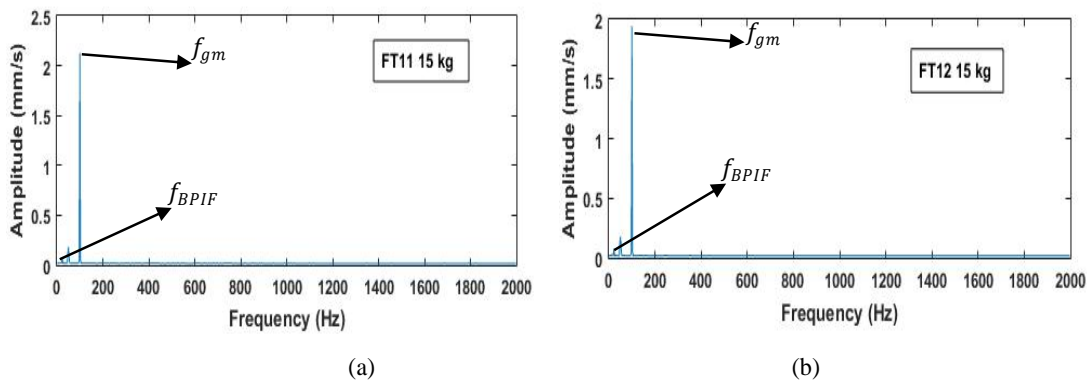
Fig. 13. Denoised frequency domain vibration response of FT11, FT12 (with an output speed of 192 rpm).

(a)   (b)
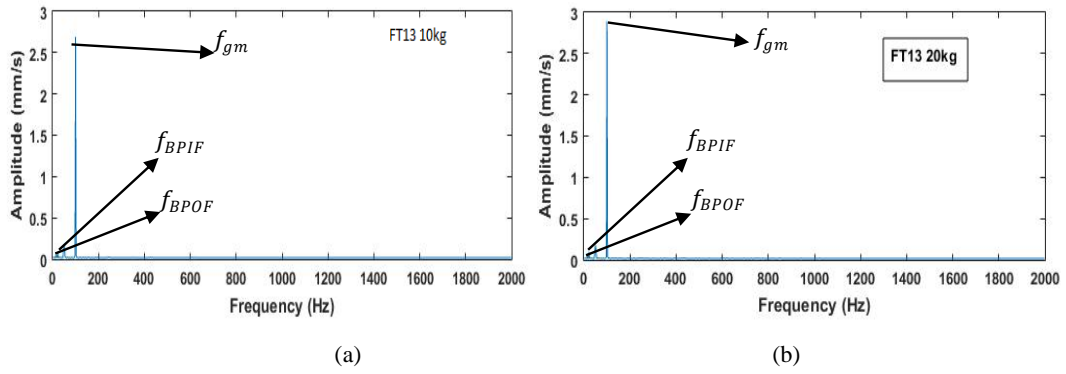
Fig. 14. Denoised frequency domain vibration response of FT13 (with an output speed of 192 rpm).

(a)   (b)
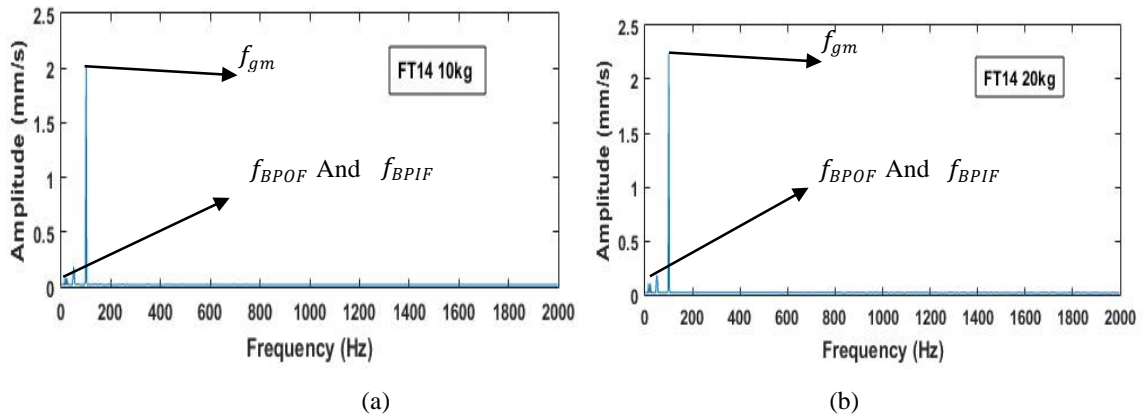
Fig. 15. Denoised frequency domain vibration response of FT14 (with an output speed of 192 rpm).

(a)   (b)
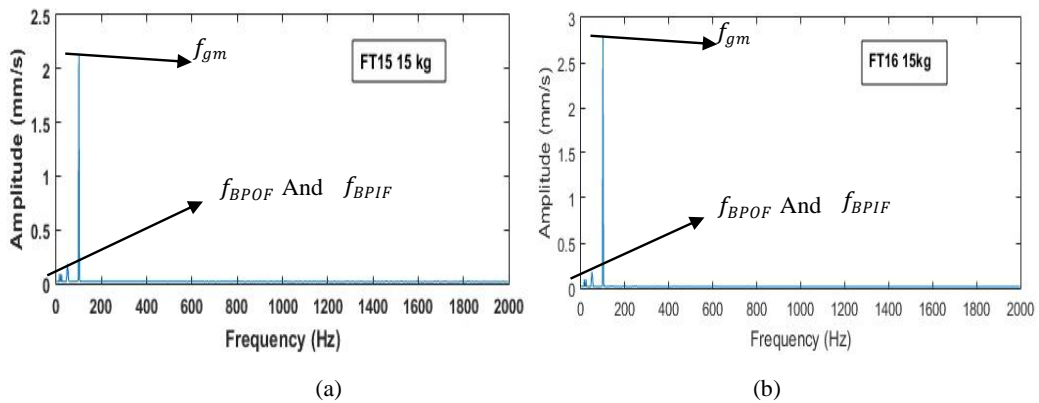
Fig. 16. Denoised frequency domain vibration response of FT15, FT16 (with an output speed of 192 rpm).

(a)   (b)
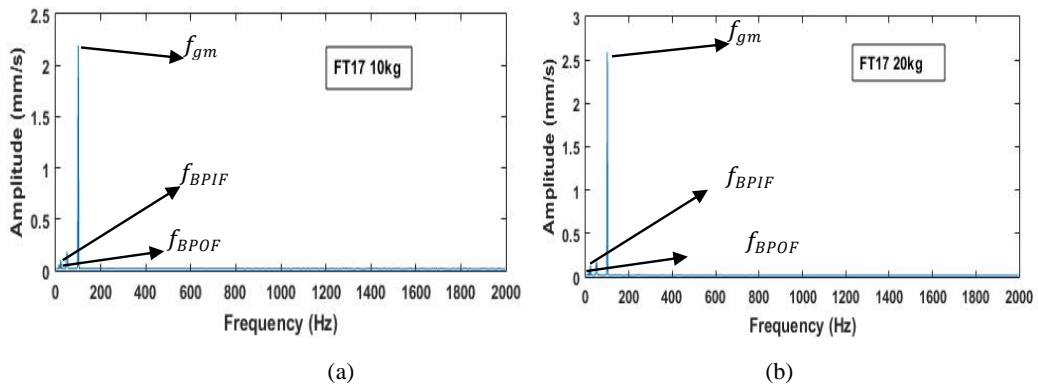
Fig. 17. Denoised frequency domain vibration response of FT17 (with an output speed of 192 rpm).

(a)

(b)
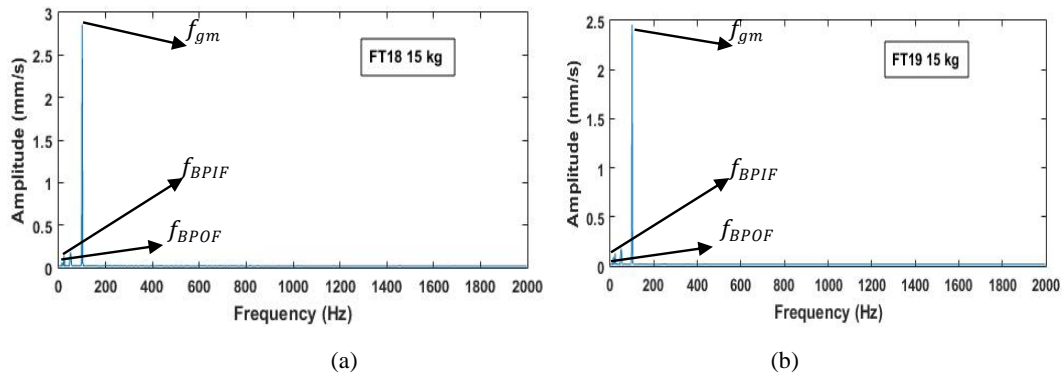
Fig. 18. Denoised frequency domain vibration response of FT18, FT19 (with an output speed of 192 rpm).

3.2 Significance from experimentation

The crucial inference that can be drawn, as depicted in Fig.19, is that the amplitude of vibration in the case of a worm gear increases abruptly with increased fault severity and load. Hence, the vibrations in the worm gear play a predominant role, and it becomes necessary to monitor the vibration levels of the worm wheel. It shows a negligible increase in the amplitude of vibration in the case of worm wheel bearings with greater stiffness.
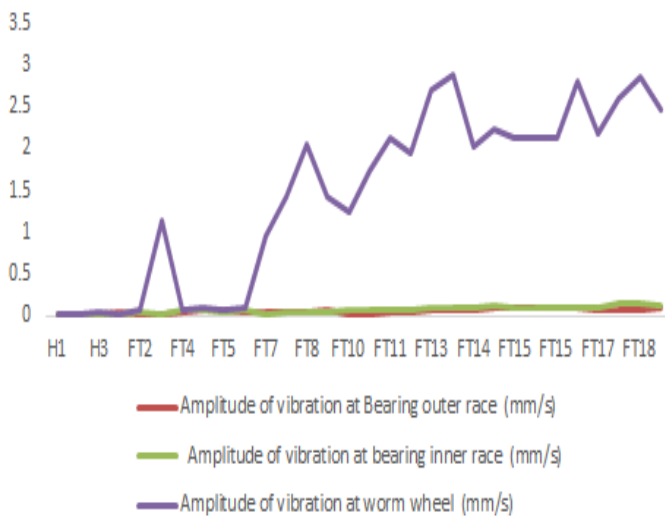
Fig. 19. Comparison of amplitude of vibration acquired from the experiments.

3.3. Performance of trained ANN

In the present work, categorisation of various faults in the worm gearbox is done by using the feed-forward-back propagation multilayer perceptron model. It works on Bayesian, scaled conjugate gradient, and Levenberg-Marquardt architectures.

3.3.1 Training of ANN depends on Bayesian architecture

The figure 20 shows the best training performance of the ANN depends on Bayesian architecture with (a) 8 hidden layers, (b) 10 hidden layers, and (c) 12 hidden layers for defect categorization. For 8, 10, and 12 hidden layer training, the ANN model stops after 631, 118, and 837 epochs, respectively, and the corresponding MSEs are 0.013679, 0.014594, and 1.3153e-13, respectively.

(a)

(b)

(c)

Fig. 20. Best training performance of ANN depends on Bayesian architecture with (a) 8 hidden layer (b) 10 hidden layer (c) 12 hidden layer for defect categorization.
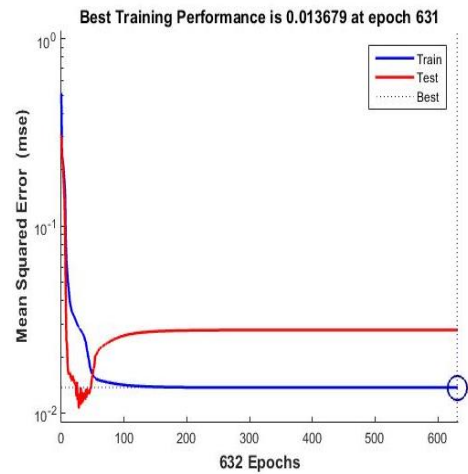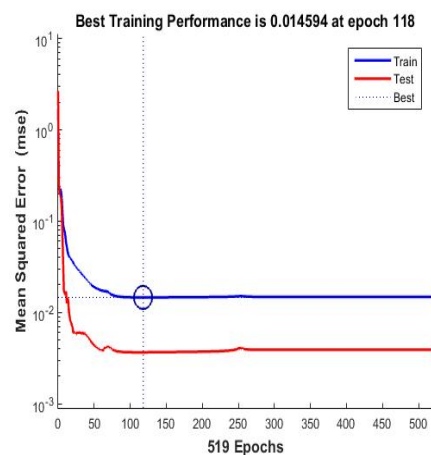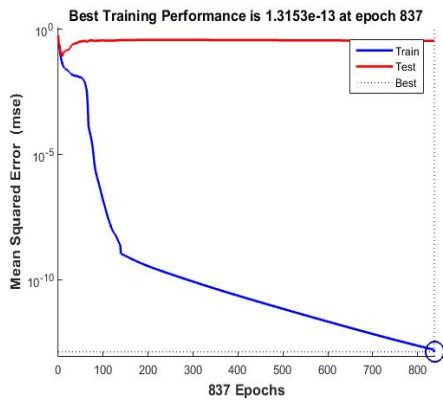
3.3.2. Training of ANN depends on scaled conjugate gradient architecture

The figure 21 shows the best training performance of ANN depends on a scaled conjugate gradient architecture with (a) 8 hidden layers, (b) 10 hidden layers and (c) 12 hidden layers for defect categorization. For 8, 10, and 12, the hidden layer training of the ANN model stops after 11, 13, and 31 epochs, respectively, and the corresponding MSEs are 0.097435, 0.026755, and 0.15266, respectively

.
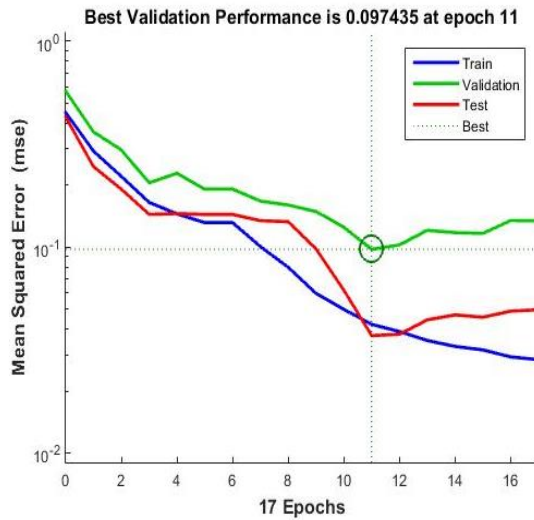
(a)
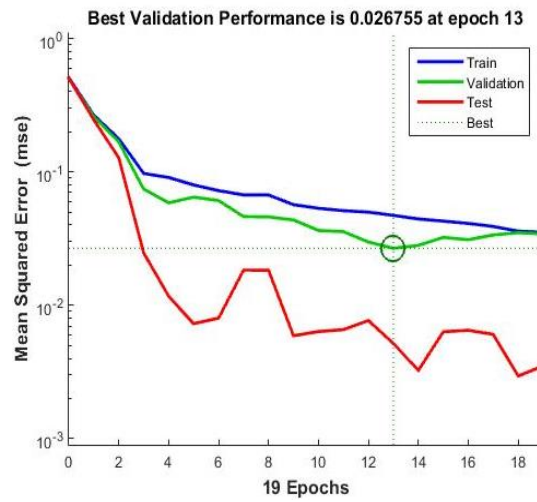
(b)
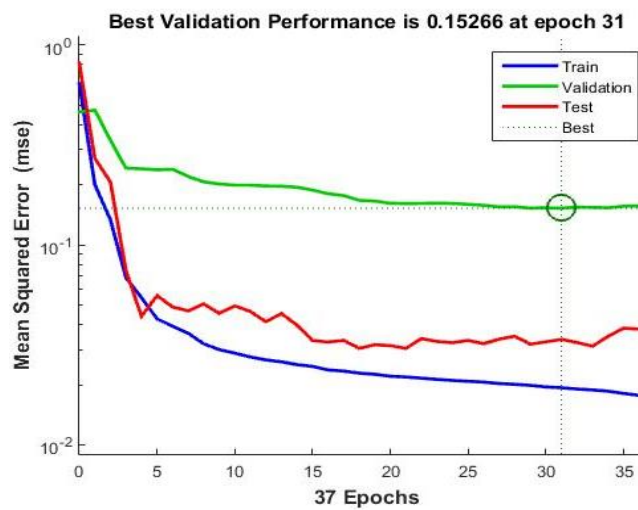
(c)

Fig. 21. Best training performance of ANN depends on scaled conjugate gradient architecture with (a) 8 hidden layer (b) 10 hidden layer (c) 12 hidden layer for defect categorization.

3.3.3. Training of ANN depends on Levenberg-Marquardt architecture

The figure 22 shows the best training performance of ANN depends on Levenberg-Marquardt architecture with (a) 8 hidden layers, (b) 10 hidden layers and (c) 12 hidden layers for defect categorization. For 8, 10, and 12 hidden layer training, the ANN model stops after 3, 4, and 2 epoch, respectively, and the corresponding MSEs are 0.13921, 0.05132, and 0.18332, respectively.
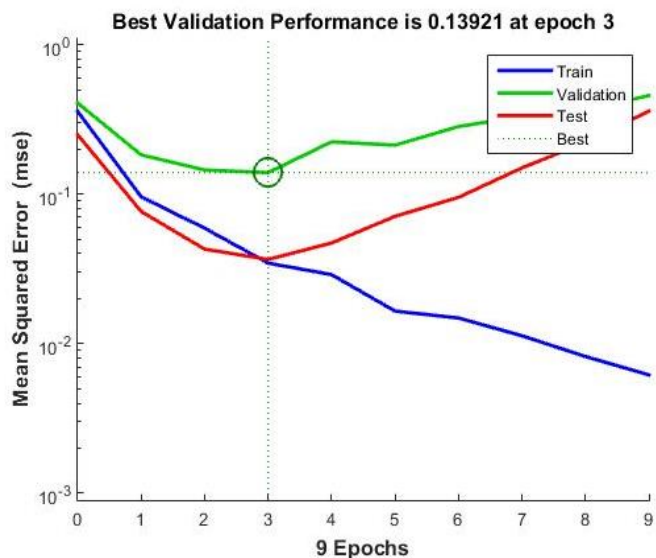
(a)
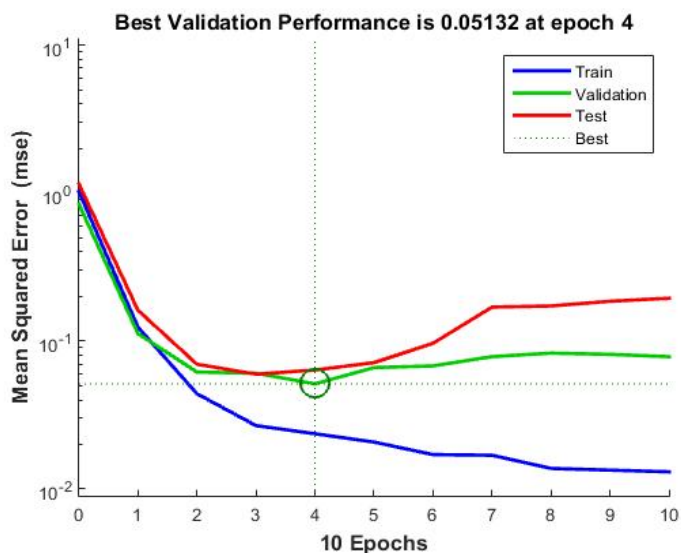
(b)
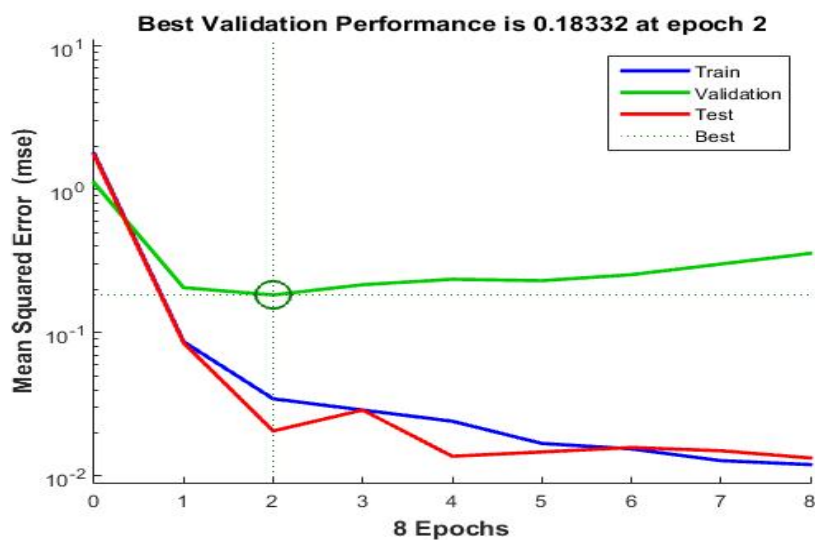
(c)

Fig. 22. Best training performance of ANN depends on Levenberg- Marquardt architecture with (a) 8 hidden layer (b) 10 hidden layer (c) 12 hidden layer for defect categorization.

A summary of the best training performance of the ANN model depends on Bayesian, scaled conjugate gradient, and Levenberg- Marquardt architectures, as mentioned in Table 3. It was found that validation data accuracy for Bayesian architecture with 8, 10, and 12 intermediate layers is zero, respectively. On the other hand, it was below 90% for the Levenberg-Marquardt architecture with 8, 10, and 12 intermediate layers, respectively. But in the case of Scaled conjugate gradient architecture validation, the data accuracy for 8 and 12 intermediate layers was below 90%, and for 10 intermediate layers, it was 94.09%, which is closer to 100% in conjunction with a mean square error (MSE) of 0.02675 at 13

epochs, which shows a close relationship between output and target. Therefore, the performance of the scaled conjugate gradient architecture with 10 hidden layers outperforms that of the Bayesian and Levenberg- Marquardt architectures. In order to categorise worm gearbox defects, an ANN model depends on the scaled conjugate gradient architecture is implemented.

Table 3. Performance of several train ANN models for defect categorization.

Architecture implemented	Intermediate layer	Epochs	Mean square error	Training data	Testing data accuracy in (%)	Validation data accuracy in (%)
Bayesian	8	631	0.01367	97.04	94.20	0
	10	118	0.01459	96.87	99.26	0
	12	837	1.3153e-13	100	41.82	0
Scaled conjugate gradient	8	11	0.09743	90.54	92.82	78.45
	10	13	0.02675	89.52	99.12	94.09
	12	31	0.1526	95.75	93.62	64.75
Levenberg-Marquardt	8	3	0.1392	92.33	94.77	74.83
	10	4	0.05132	94.78	85.76	88.88
	12	2	0.1833	92.29	94.85	61.62

3.4. Prediction potential of ANN

Categorising worm gearbox defects using ANN basically depends on the confusion matrix. The confusion matrix includes output and target. In current research, an ANN model that depends on scaled conjugate gradient architecture was trained for categorising worm gearbox defects. To achieve solidity in defect categorisation, the scaled conjugate gradient architecture was trained five times. To categorise worm gearbox defects, four outputs are considered: a good worm gearbox, a defect on the inner and outer race, a broken tooth, and an integrated fault on the worm gear and bearing in conjunction with the target: (1,0,0,0), (0,1,0,0), (0,0,1,0), and (0,0,0,1), respectively. The confusion matrix consists of four matrix, such as training, testing, validation, and the overall confusion matrix. Out of the total data, the training confusion matrix categorises 70% of the data, and the testing and validation confusion matrix categorises 15% of the data. On the other hand, overall confusion matrix categorises 100% of the data.

Table 4 indicates the effectiveness of the scaled conjugate gradient architecture ANN model for defect categorisation with 10 hidden layers. The accuracy given by the overall confusion matrix for defect categorization was 97.6%, 100%, 95.2%, 95.2%, and 97.6%. Similarly, the cross-entropy recorded was 0.0091, 3.2221e-09, 0.004228, 2.0311e-06, and 9.8661e-07. These values are somewhat different. The obtained results demonstrate that for the second trial, the ANN model, which depends on the scaled conjugate gradient with 10 hidden layers, provides high solidity and reliability for categorising worm gearbox defects. The confusion matrix and best validation performance from the second experiment are displayed in Figs. 23 and 24, respectively.

Table 4. Effectiveness of scaled conjugate gradient architecture ANN model for defects categorisation with 10 hidden layer.

Trial No.	Epochs	Cross entropy	Accuracy on training confusion matrix (%)	Accuracy on testing confusion matrix (%)	Accuracy on validation confusion matrix (%)	Accuracy on all confusion matrix (%)
1	17	0.0091	96.7	100	100	97.6
2	30	3.2221e-09	100	100	100	100
3	10	0.004228	96.7	83.3	100	95.2
4	48	2.0311e-06	100	66.7	100	95.2
5	37	9.8661e-07	100	83.3	100	97.6
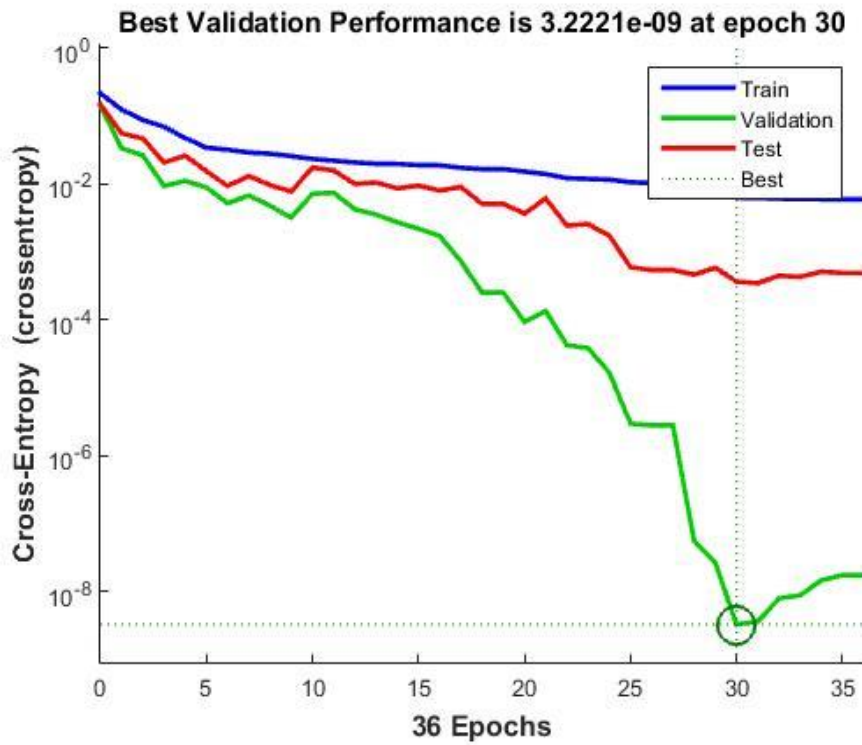
Fig. 23. Optimal testing outcomes for the second trial.

Fig. 24. The second trial, a confusion matrix.

3.5. Comparison and discussion with some earlier published works

Table 5. Comparison of the current findings with earlier worm gearbox studies.

Published work	Methods for monitoring	DOE considered	Statistician-extracted features	Defect considered	Coalesce defect considered
[17]	Temperature	No	No	Broken of a single worm wheel teeth	NO
[20]	Acoustic emission	No	RMS, kurtosis	Teeth of a single worm wheel encountered pitting	NO
[21]	Vibration	No	RMS	Defective inner and outer wheel bearing races	NO
[22]	Vibration	No	Mean, Median, RMS, standard deviation , peak to peak, crest factor, skewness and kurtosis	The teeth of several worm gears were pitted	NO
Current work	Vibration	Yes	The sample variance, RMS, crest factor, kurtosis, mean, peak to peak, skewness, and standard deviation	Teeth breakage in the worm wheel, scratch on the inner and outer races of the bearings, and the combination of all three	Yes

Table 5 illustrates a comparison of current research with the worm gearbox literature that has been published. Vibration monitoring is used to evaluate the coalesced, or combined, worm wheel and bearing defect, but no work has been found to be reported on this matter. Similarly, none of the published work is found with the implementation of DOE to plan systematic experimental trials. The primary benefit of the current study is that it offers an experimental examination together with a practical technique for defect identification in worm gearboxes with coalesced faults. Thermal analysis would successfully identify a single broken worm wheel tooth without extracting statistical data, according to Babu et al. [17].

The pitting problems on the worm wheel can be prominently identified by acoustic emission based RMS and kurtosis, as per the findings of Elforjani et al. [20]. Elasha et al. [21] found that the vibration based RMS response can be useful for fault detection in worm wheel and bearing races. As per the findings of Umutu et al. [22], the diagnosis of pitting on a worm wheel using ANN improves with the extraction of statistical parameters. The present work utilized an ANN model based on a scaled conjugate gradient architecture for fault categorization. The results show that the present model, which depends on a scaled conjugate gradient, is capable of making the predictions with fair accuracy.

3.6. Comparison of ANN model with support vector machine (SVM)

The SVM model is developed using various ribbon blender worm gearbox conditions (see Table 2) and eight frequency domain vibration response statistical parameters: standard deviation, variance, skewness, peak to peak, kurtosis, RMS, mean, and crest factor. From the available literature, John Platt's sequential algorithm is implemented for training SVM [4, 23]. The SVM model is trained utilising the MATLAB classifier toolbox. 8-fold cross-validation is implemented to produce training data for SVM model development. The complexity parameter is set to 100. A linear kernel function is used for analysis. Fig. 25 shows the confusion matrix for the trained SVM. Fig. 25 (a) and (b) are useful to observe the accuracy of the pre-true class, i.e, training class and the pre-predicted class, i.e, the testing class. The SVM model's overall accuracy is depicted in Fig. 25(c). The trained SVM model has an overall accuracy of 92.9% and a 7.1% overall error. Based on overall accuracy, the ANN model is compared with the SVM model, as mentioned in Table 6.

Table 6. Comparison of ANN with SVM.

Machine learning tool	Over all accuracy	Over all error
ANN	97.12 %	1.02 %
SVM	92.9 %	7.1 %
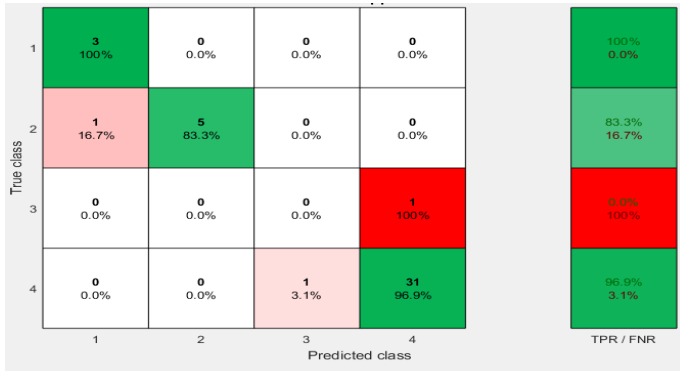
(a) Pre true confusion matrix
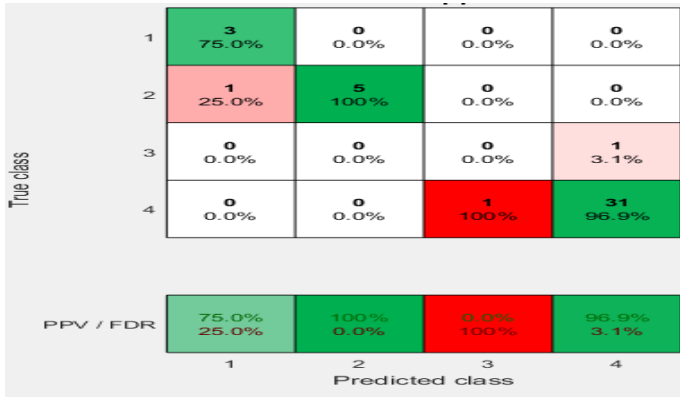
(b) Pre predicted confusion matrix
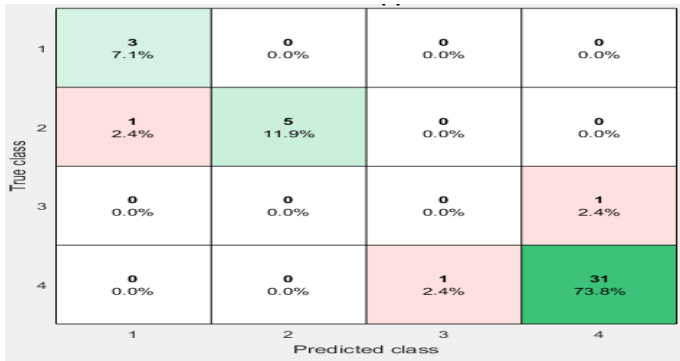
(c) Over all confusion matrix

Fig. 25. Confusion matrix for the SVM model.

4. Conclusions

This work presents a technique for coalescing defect, i.e., the effect of defects at a time in the worm wheel, bearing inner race and outer race categorization in the worm gear box. The experimental trials were performed to acquire vibration signatures. The wavelet denoising method is implemented to reconstruct the contaminated vibration signatures. The statistical parameters like standard deviation, variance, skewness, peak to peak, kurtosis, RMS, mean, and crest factor are influential and captured during the experiments. Further, it proposes the use of ANN and SVM. Using the captured data, the models of ANN and SVM are trained, which further categorizes the defects. Based on the inferences drawn from the study, subsequent conclusions have been drawn:

1) To identify faults present in the worm gearbox by using vibration signatures, characteristics rotational frequencies, those are gear mesh frequency (f_{gm}), bearing pass outer race frequency (f_{BPOF}), bearing pass inner race frequency (f_{BPIF}), which are strong predictors of worm wheel and bearing faults.

2) The performance of the gearbox deteriorates with the presence of the defect. The defect on the inner bearing race prominently rises the vibration level as compared to the defect on the outer race. Hence, the bearing inner race defect is predominant as compared to the bearing outer race.

3) The defect categorization can be done with the scaled conjugate gradient architecture in ANN and John Platt's sequential architecture in SVM. Based on overall accuracy, the ANN model is superior to SVM in classifying worm gearbox defects.

4) The study's findings suggest that the technique was sound, successfully increased productivity, dependability, and efficiency, and reduced maintenance costs.

References

1. Dhamande L S, Chaudhari M B. Compound gear-bearing fault feature extraction using statistical features based on time-frequency method, Measurement 2018; (125): 63–77. https://doi.org/10.1016/j.measurement.2018.04.059

2. Ammar D M, Oraby S E, Younes M A, Elsayed S. E. Prediction of bearing service life using an auto regression moving average and response surface methodology, Applications of Modelling and Simulation 2022; (6): 1-9, http://arqiipubl.com/ojs/index.php/AMS_Journal/article/view/324/128

3. Tang X, Xu Y, Sun X, Liu Y, Jia Y, Gu F, Ball A D. Intelligent fault diagnosis of helical gearboxes with compressive sensing based non-contact measurements, ISA Transactions 2022; (20): 1-16, https://doi.org/10.1016/j.isatra.2022.07.020

4. Chen Z, Cen J, Xiong J. Rolling bearing fault diagnosis using time-frequency analysis and deep transfer convolutional neural network, Access 2020; (8): 150248-150261, https://ieeexplore.ieee.org/document/9167237, https://doi.org/10.1109/ACCESS.2020.3016888

5. Alshammari S A M, Makrahy M M, Ghazaly N M. Fault diagnosis of helical gear through various vibration techniques in automotive gearbox, Journal of Mechanical Design and Vibration 2019; (7): 21-26, http://www.sciepub.com/JMDV/abstract/10727

6. Sharma V. A review on vibration-based fault diagnosis techniques for wind turbine gearboxes operating under nonstationary conditions, J. Inst. Eng. India Ser. C 2021; (102): 507–523. https://link.springer.com/article/10.1007/s40032-021-00666-y

7. Teng W, Ding X, Cheng H, Han C, Liu Y, Mu H. Compound faults diagnosis and analysis for a wind turbine gearbox via a novel vibration model and empirical wavelet transform, Renewable Energy 2019; (136), 393-402, https://doi.org/10.1016/j.renene.2018.12.094

8. Chen A, Kurfess T R. A new model for rolling element bearing defect size estimation. Measurement, 2018; (114): 144-149, https://doi.org/10.1016/j.measurement.2017.09.018.

9. Goyal D, Choudhary A, Sandhu J K, Srivastava P, Saxena K K. An intelligent self-adaptive bearing fault diagnosis approach based on improved local mean decomposition, Int J Interact Des Manuf 2022; (72), https://doi.org/10.1007/s12008-022-01001-0

10. Miao F, Zhao R., Wang X. A new method of denoising of vibration signal and its application, Shock and Vibration, 2020; (2): 1-8, https://doi.org/10.1155/2020/7587840

11. Liu Z, Zhang L, Carrasco J. Vibration analysis for large-scale wind turbine blade bearing fault detection with an empirical wavelet thresholding method, Renewable Energy 2020; (146)P: 99-110, https://doi.org/10.1016/j.renene.2019.06.094

12. Miao F, Zhao R. A new fault diagnosis method for rotating machinery based on SCA-FastICA, Shock and Vibration, 2020; (2): 1-12. https://doi.org/10.1155/2020/6576915.

13. Xu A, Huang W, Li P, Chen H, Meng J, Guo X. Mechanical vibration signal denoising using quantum-inspired standard deviation based on subband based gaussian mixture model, Shock and Vibration 2018; 1-9, https://doi.org/10.1155/2018/5169070.

14. Mishra C, Samantaray A K, Chakraborty G. Rolling element bearing fault diagnosis under slow speed operation using wavelet de-noising, Measurement 2017; (103): 77-86, https://doi.org/10.1016/j.measurement.2017.02.033

15. Hizarci B, Umutlu R C, Kiral Z, Ozturk H. Vibration region analysis for condition monitoring of gearboxes using image processing and neural networks. Experimental Techniques, 2019; (43): 739-755, https://doi.org/10.1007/s40799-019-00329-9

16. Karabacak Y E, Ozmen N G, Gumusel L. Worm gear condition monitoring and fault detection from thermal images via deep learning method. Maintenance and Reliability, 2020; (22): 544–556, http://dx.doi.org/10.17531/ein.2020.3.18

17. Babu T N, Patel D, Tharnari D, Bhatt A. Temperature behavior-based monitoring of worm gears under different working conditions, Innovative Design, Analysis and Development Practices in Aerospace and Automotive Engineering 2019; (2): 257-265, DOI:10.1007/978-981-13-2718-6_24

18. Chothani H G, Maniya K D. Experimental investigation of churning power loss of single start worm gear drive through optimization technique, Materials Today Proceedings 2020; (28) 2031-2038, https://doi.org/10.1016/j.matpr.2019.12.365

19. Hizarci B, Umutlu R C, Kiral Z, Ozturk H. Fault severity detection of a worm gearbox based on several feature extraction methods through a developed condition monitoring system, SN Applied Sciences 2021; 3(1): 129-140, https:// DOI:10.1007/s42452-020-04131-w

20. Elforjani M, Mba D, Muhammad A, Sire A. Condition monitoring of worm gears, Applied Acoustics 2012; (73): 859–863, https://doi.org/10.1016/j.apacoust.2012.03.008

21. Elasha F, Cárcel C R, Mba D, Kiat G, Nze I, Yebra G. Pitting detection in worm gearboxes with vibration analysis, Engineering Failure Analysis 2014; (42): 366-376, https:// DOI:10.1016/j.engfailanal.2014.04.028.

22. Umutlu R C, Hizarci B, Kiral Z, Ozturk H. Classification of pitting fault levels in a worm gearbox using vibration visualization and ANN, Sadhana Academy Proceedings in Engineering Sciences 2020; (45): 1-13, https:// doi.org/10.1007/s12046-019-1263

23. Tyagi S, Panigrahi S K. An SVM—ANN hybrid classifier for diagnosis of gear fault, Applied Artificial Intelligence 2017; (31): 209-231. https://doi.org/10.1080/08839514.2017.1315502

24. Barshikar R R, Baviskar P R. Evaluation of performance of vibration signatures for condition monitoring of worm gearbox by using ANN, International Journal on Interactive Design and Manufacturing 2023; (62): 1-14, https://doi.org/10.1007/s12008-023-01268-x

25. Agrawal P, Jayaswal P. Diagnosis and classifications of bearing faults using artificial neural network and support vector machine, J. Inst. Eng. India Ser. C, 2019; (101): 61–72, https://doi.org/10.1007/s40032-019-00519-9

26. Karpat F, Kalay O C, Dirik A E, Karpat E. Fault classification of wind turbine gearbox bearings based on convolutional neural networks, Transdisciplinary Journal of Engineering & Science 2022; (2): 71-83, https://orcid.org/0000-0001-8474-7328

27. Niaki S T, Alavi H, Ohadi A. Incipient fault detection of helical gearbox based on variational mode decomposition and time synchronous averaging, Structural Health Monitoring 2022; (5): 21-31. https://doi.org/10.1177/14759217221108489

28. Kane P V, Andhare A B. Critical Evaluation and comparison of psychoacoustics, acoustics and vibration features for gear fault correlation and classification, Measurement (2020); (154): 1-28, https://doi.org/10.1016/j.measurement.2020.107495

29. Attoui I, Fergani N, Boutasseta N, Oudjani B, Deliou A. A new time–frequency method for identification and classification of ball bearing faults, Journal of Sound and Vibration 2017; (397): 241-265, https://doi.org/10.1016/j.jsv.2017.02.041

30. Dabrowski D. Condition monitoring of planetary gearbox by hardware implementation of artificial neural networks, Measurement 2016; (91): 295-308, https://doi.org/10.1016/j.measurement.2016.05.056

31. Ammar D M, Oraby S E, Younes M A, Elsayed S E. Prediction of bearing service life using an auto regression moving average and response surface methodology, Applications of Modelling and Simulation 2022; (6): 1-9, http://arqiipubl.com/ojs/index.php/AMS_Journal/article/view/324/128

32. Mishra H P, Jalan A. Analysis of faults in rotor-bearing system using three-level full factorial design and response surface methodology Noise & Vibration Worldwide 2021; (52): 1-12, https://DOI: 10.1177/09574565211030711

33. Vanraj, Dhami S S, Pabla B S. Optimization of sound sensor placement for condition monitoring of fixed-axis gearbox, Cogent Physics 2017; (4), 1-19, https://dx.doi.org/10.1080/23311916.2017.1345673

34. Goyal D, Vanraj, Pabla, B S, Dhami S S. Non-contact sensor placement strategy for condition monitoring of rotating machine-elements, Engineering Science and Technology, an International Journal 2019; (22): 489-501, https://doi.org/10.1016/j.jestch.2018.12.006